



## A magnetic anomaly associated with an albedo feature near Airy crater in the lunar nearside highlands

D. T. Blewett,<sup>1,2</sup> B. R. Hawke,<sup>3</sup> N. C. Richmond,<sup>4,5</sup> and C. G. Hughes<sup>6</sup>

Received 16 August 2007; revised 9 October 2007; accepted 22 October 2007; published 27 December 2007.

[1] We describe a strong crustal magnetic anomaly, recently identified in Lunar Prospector magnetometer data, that is associated with a previously unreported albedo feature near the crater Airy in the lunar nearside highlands. Other workers have demonstrated a correlation between magnetic anomalies and the enigmatic bright markings known as lunar swirls. We have used Earth-based telescopic spectra and Clementine multispectral images to investigate the compositional and optical maturity characteristics of the Airy swirl. The Airy albedo feature does not exhibit the complex sinuous structure of well-known swirls such as the Reiner Gamma Formation, but does possess a bright loop and central dark lane. Another strong magnetic anomaly, in the Apollo 16/Descartes region, corresponds to a simple diffuse bright albedo spot. On this basis we suggest that a continuum of swirl morphologies exists on the Moon, with the Airy feature representing an intermediate or incipient swirl form. **Citation:** Blewett, D. T., B. R. Hawke, N. C. Richmond, and C. G. Hughes (2007), A magnetic anomaly associated with an albedo feature near Airy crater in the lunar nearside highlands, *Geophys. Res. Lett.*, 34, L24206, doi:10.1029/2007GL031670.

### 1. Introduction

[2] Lunar swirls are unusual bright markings found in both the maria and the highlands [El-Baz, 1972; Schultz and Srnka, 1980; Bell and Hawke, 1981]. These sinuous high albedo patches sometimes exhibit dark lanes between bright segments. Swirls have no apparent topographic expression and appear to overprint the surfaces on which they lie. Several origins for lunar swirls have been proposed. An association between swirls and magnetic anomalies has been reported [e.g., Hood et al., 2001, and references therein], which has led to the hypothesis that the magnetic anomaly protects the surface from the solar wind [e.g., Hood and Schubert, 1980; Hood and Williams, 1989; Hood et al., 2001]. Lacking solar wind sputtering and implantation, the regolith does not undergo the normal soil-darkening process (“space weathering”) to which unshielded areas

are subjected. Thus it may be that the presence of a magnetic anomaly specially preserves a high albedo, even though a magnetically shielded surface would still experience micrometeorite bombardment. Micrometeorite impact is thought to play a major role in space weathering by producing melting, agglutinate formation, and vapor deposition among regolith grains [e.g., Hapke, 2001; Noble and Pieters, 2003]. A number of magnetic anomalies are correlated with terranes antipodal to the major impact basins [Lin et al., 1988; Richmond et al., 2005]. Numerical models of lunar basin formation suggest that these anomalies originated as a consequence of impact shock or rapid thermal magnetization in the presence of an amplified field [e.g., Hood and Artemieva, 2007], and transient field enhancements associated with basin formation may also explain magnetic anomalies that are not antipodal to major basins. The correlation of magnetic anomalies with basin antipodes implies that the shielding has been operating since the time of basin formation ( $> \sim 3.8$  billion years), and hence that the swirls are very old features. However, over time crater-forming impacts could contribute new ejecta material to a magnetically shielded area, occasionally “refreshing” the swirl.

[3] Alternate mechanisms hypothesized for the formation of lunar swirls involve surface effects produced during the relatively recent ( $< \sim 1$  Myr) impact of meteor swarms [Starukhina and Shkuratov, 2004], a comet coma and nucleus [Schultz and Srnka, 1980], or disrupted comet fragments [Pinet et al., 2000]. Nicholas et al. [2007] modeled the source of the magnetic anomaly at the Reiner Gamma Formation (RGF), the type example of a lunar swirl, and found that the thickness and strength of the magnetized unit are more consistent with a layer of magnetized basin ejecta than with a thin surficial deposit produced by comet or meteoroid impact.

[4] A new analysis of Lunar Prospector magnetometer data collected during the spacecraft’s low-altitude orbital phase [Richmond and Hood, 2007; Richmond et al., 2005] is providing magnetic maps for portions of the Moon for which coverage was previously unavailable. In this paper we report on a strong magnetic anomaly in the lunar nearside highlands, in the vicinity of Airy crater (Airy crater is centered at  $\sim 18.1^\circ$  S,  $5.7^\circ$  E). We investigate the spectral and compositional properties of an albedo feature associated with the Airy magnetic anomaly. We also describe a progression in the morphology of albedo markings linked to lunar magnetic anomalies.

### 2. Data

[5] We have been conducting an integrated study of lunar swirls. Clementine multispectral images calibrated to reflectance

<sup>1</sup>NovaSol, Honolulu, Hawaii, USA.

<sup>2</sup>Now at John Hopkins University Applied Physics Laboratory, Laurel, Maryland, USA.

<sup>3</sup>Hawai’i Institute of Geophysics and Planetology, University of Hawai’i at Manoa, Honolulu, Hawaii, USA.

<sup>4</sup>Planetary Science Institute, Tucson, Arizona, USA.

<sup>5</sup>Lunar and Planetary Laboratory, University of Arizona, Tucson, Arizona, USA.

<sup>6</sup>Department of Geology and Planetary Science, University of Pittsburgh, Pittsburgh, Pennsylvania, USA.

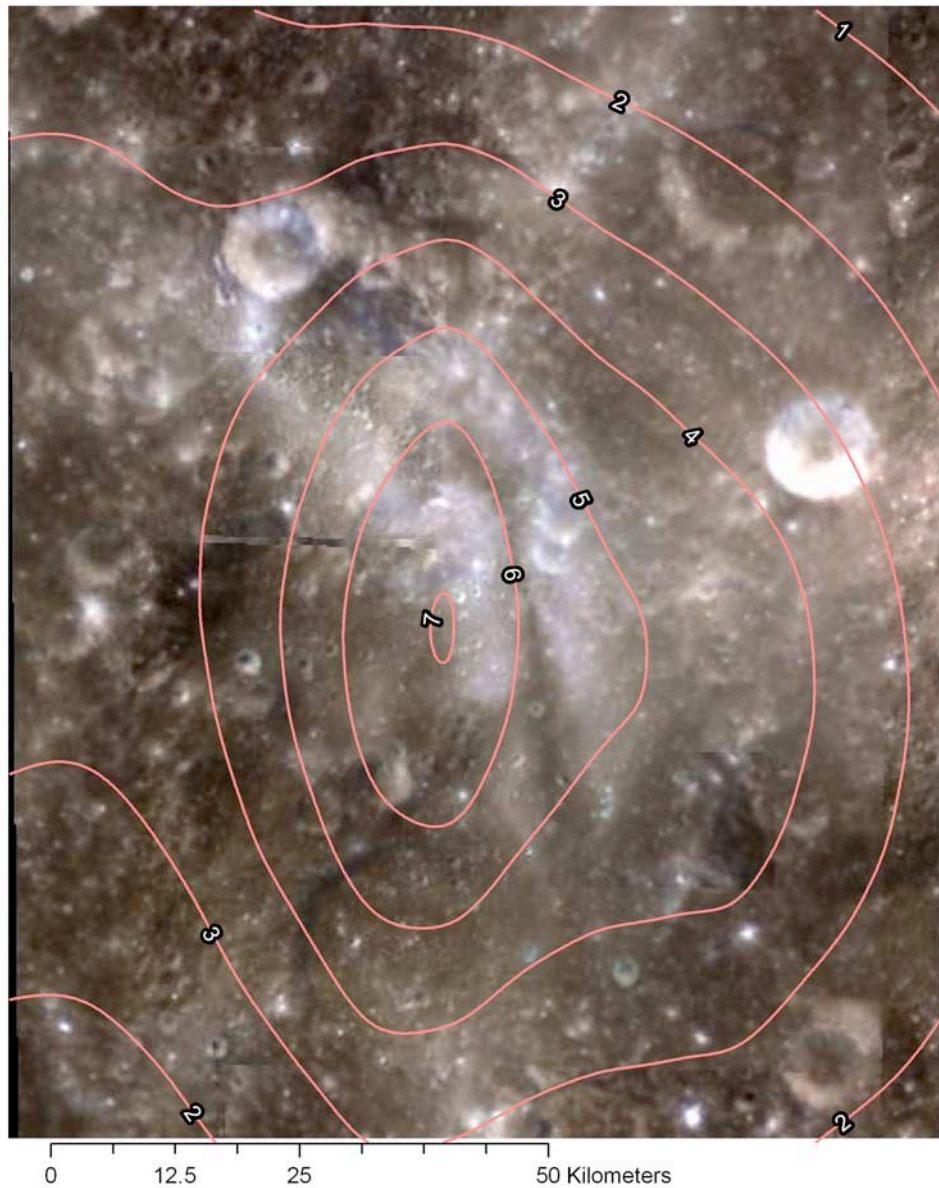


**Figure 1.** Clementine image mosaic for the Airy magnetic and albedo anomaly, in sinusoidal projection. Contours of Lunar Prospector two-dimensionally smoothed total magnetic field strength at 35.5 km altitude are labeled in nT. The image is centered at 18.1°S, 3.25°E; north is to the top. The Airy albedo anomaly is the bright area in the center of the image. Refer to Figure 2 for a context view with lighting conditions that emphasize topography.

tance can be used to produce a number of spectral parameter maps, including relative color (415-nm/750-nm ratio), optical maturity (OMAT) [Lucey *et al.*, 2000b; Grier *et al.*, 2001], and iron and titanium content [e.g., Lucey *et al.*, 2000a]. Data from the Lunar Prospector magnetometer experiment has been continued to a common altitude of 35.5 km for selected areas [Richmond and Hood, 2007; Richmond *et al.*, 2005]. Figure 1 presents a Clementine base image for the vicinity of Airy crater with Lunar Prospector total magnetic field contours.

[6] Earth-based telescopic spectra in the near-infrared (NIR,  $\sim 0.6\text{--}2.5\ \mu\text{m}$ ) provide information on the composition and state of maturity of the surface [e.g., McCord *et al.*, 1981]. Four NIR spectra for features related to the Airy albedo feature were obtained under favorable observing

conditions. The projected spot size of the spectrometer aperture on the lunar surface was  $\sim 2$  km in diameter. The spot locations, shown in Figure 2, include a portion of the albedo anomaly (“Swirl”), the interior of crater Argelander D, the floor of Airy crater, and the very fresh small crater Airy M. Reflectance spectra are shown in Figure 3, along with relative spectra produced by dividing out a straight-line continuum. The continuum-removed spectra allow detailed comparison of the shapes of the absorption band near  $1\ \mu\text{m}$  caused by  $\text{Fe}^{2+}$  in mafic minerals.

### 3. Analysis

[7] The crustal magnetic anomaly near Airy has a two-dimensionally smoothed peak total field strength at 35.5 km

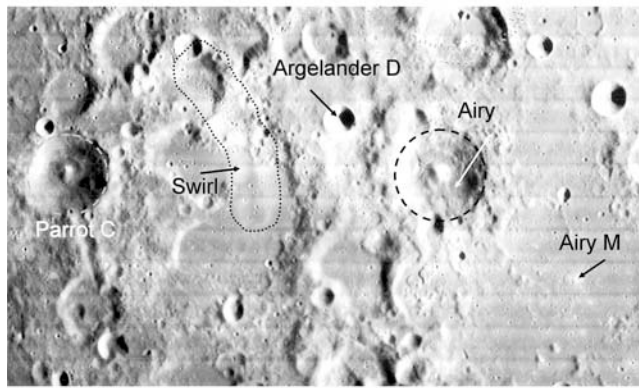


**Figure 2.** Portion of Lunar Orbiter IV frame 101-H2 showing the vicinity of Airy crater. North is to the top. Airy crater is  $\sim 37$  km in diameter. Arrows mark locations for which the telescopic near-infrared spectra of Figure 3 were collected; spot sizes were  $\sim 2$  km in diameter. The swirl-like albedo feature is indicated by the dotted outline; compare to the Clementine image shown in Figure 1.

altitude of  $\sim 7$  nT. The Reiner Gamma Formation is also co-located with a magnetic anomaly whose smoothed total

peak strength when continued to 35.5 km altitude is 7 nT (Figure 4). The RGF 4-nT contour covers an area  $\sim 87 \times 110$  km in size; at Airy the 4-nT contour is  $\sim 60 \times 70$  km. Thus, the Airy magnetic anomaly is similar in magnitude, though smaller in spatial extent, to one of the strongest and best known of the lunar crustal magnetic anomalies. The spatial extent of the RGF swirl marking is quite large, extending several hundred kilometers across the dark mare basalts of Oceanus Procellarum, compared to the Airy albedo feature whose long dimension is  $\sim 50$ – $60$  km.

[8] The NIR reflectance spectra shown in Figure 3 are somewhat noisy, but the quality is sufficient for interpretation. We applied the analysis techniques described by *Lucey et al.* [1986] and *Blewett et al.* [1995]. The aims of the spectral analysis are to determine the mineralogy and lithology of the Airy albedo anomaly, and to compare with results for nearby fresh and mature highland material. The spectral parameters derived for the group of Airy-related spectra are listed in Table 1. The NIR continuum slope ( $\Delta(\text{reflectance})/\Delta(\text{wavelength})$ ) is controlled by both composition and maturity, with higher-FeO and/or more mature surfaces having spectra with steeper (higher) continuum slopes. The NIR continuum slope is measured by fitting a straight line to tangent points on a spectrum on either side of

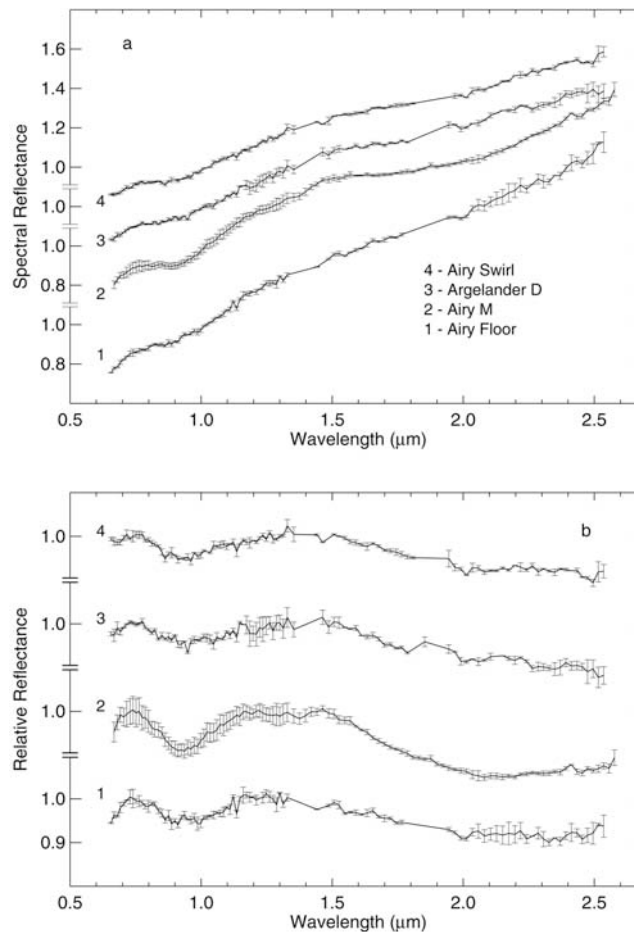


**Figure 3.** Telescopic NIR spectra for locations shown in Figure 2. (a) Reflectance spectra. Spectra are scaled to a value of 1.0 at  $1.02 \mu\text{m}$ , and have been offset for clarity. Portions of the spectra in the vicinity of telluric water vapor absorptions have been omitted. (b) Continuum-removed spectra, illustrating the characteristics of the  $\text{Fe}^{2+}$  absorption band centered near  $1 \mu\text{m}$ .

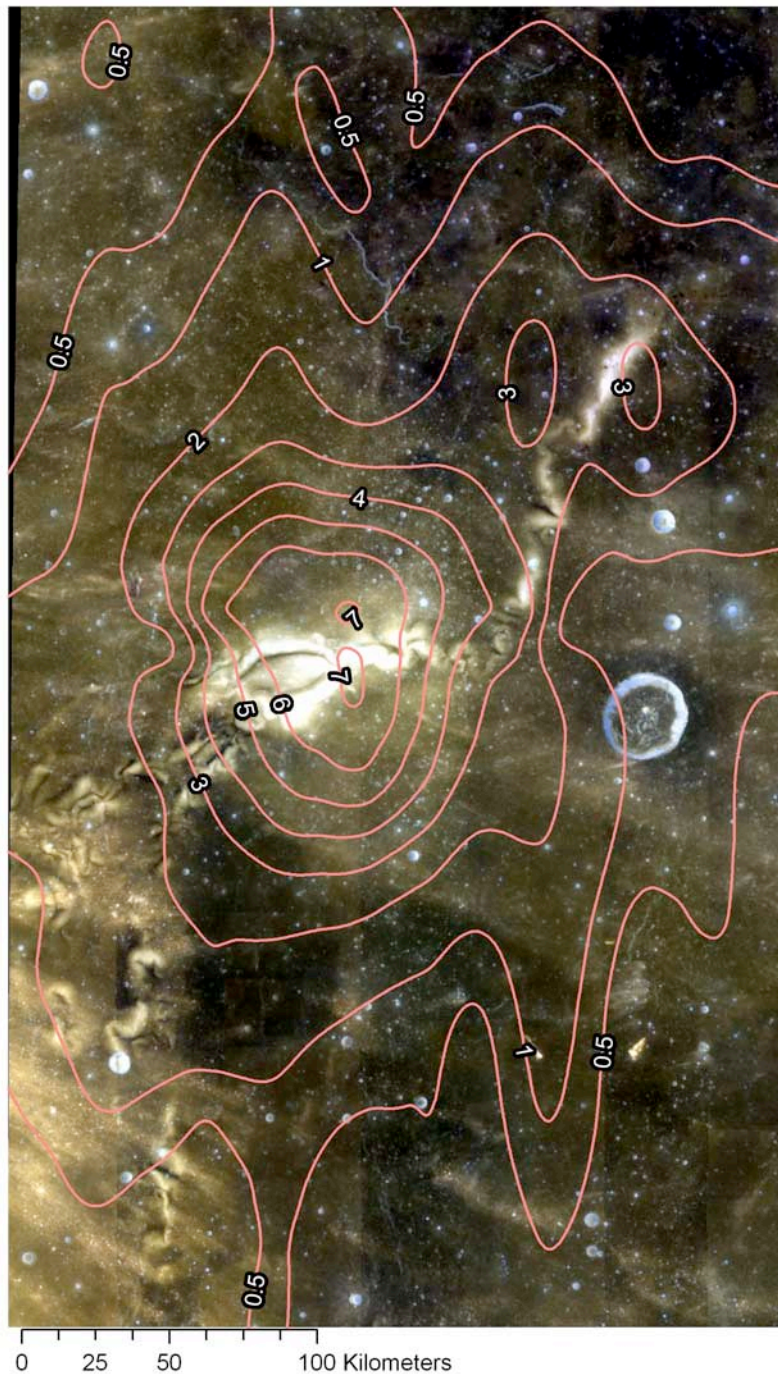


**Figure 4.** The Reiner Gamma Formation, the type occurrence of a lunar swirl. The Clementine image mosaic centered at  $7.5^{\circ}\text{N}$ ,  $302.5^{\circ}\text{E}$  is in sinusoidal projection, with contours of Lunar Prospector two-dimensionally smoothed total magnetic field strength at 35.5 km altitude. North is to the top. Contour lines are labeled in nT.

the “1  $\mu\text{m}$ ” band. Of principal interest for determining mineralogy are the wavelength position of the band minimum and the band depth. These parameters are determined by performing fits to a spectrum that has been divided by the continuum (the “continuum-removed” spectrum). High-Ca pyroxenes (clinopyroxenes) give rise to spectra with band minima at wavelengths  $>0.95 \mu\text{m}$ . Low-Ca pyroxenes are characterized by band minima shortward of  $0.95 \mu\text{m}$ . Surfaces with a greater abundance of pyroxene or with higher-Fe pyroxenes will have deeper absorption bands.

The uncertainty in the spectral parameters is partly determined by the quality of the spectrum being analyzed. For the spectra with the poorest precision discussed here, we estimate the maximum uncertainties to be  $\pm 0.05 \mu\text{m}^{-1}$  in slope,  $\pm 0.01 \mu\text{m}$  in the position of the band minimum, and  $\pm 1\%$  in depth.

[9] The telescopic spectral results indicate that feldspathic lithologies are present at all the locations that were observed. The mafic mineral assemblages are dominated by low-Ca pyroxene. Differences in the spectral parameters for

**Table 1.** Spectral Parameters Determined for the NIR Spectra Shown in Figure 3

Spectrum	Slope, <sup>a</sup> $\mu\text{m}^{-1}$	Min, <sup>b</sup> $\mu\text{m}$	Depth, <sup>c</sup> %
1 Airy Floor	0.67	0.94	5.1
2 Airy M	0.61	0.93	8.9
3 Argelander D	0.50	0.95	4.3
4 Airy Swirl	0.46	0.94	5.1

<sup>a</sup>NIR spectral slope.<sup>b</sup>Wavelength position of band minimum.<sup>c</sup>Depth of “1  $\mu\text{m}$ ” band.

the locations observed (Table 1) are caused by maturity differences, and to a much lesser extent, minor variations in mafic mineral abundance. The rock type corresponding to the composition found in the floor of Airy crater and at Airy M is anorthositic norite (terminology of *Stöffler et al.* [1980]). The lithology at the other two locations that were observed is slightly less mafic, and corresponds to noritic anorthosite. Clementine compositional maps reveal that the albedo anomaly has an FeO content of  $\sim 7\text{--}8$  wt.%, and TiO<sub>2</sub> of  $<1$  wt.%. Surrounding highland surfaces have FeO  $\sim 6\text{--}9$  wt.% and TiO<sub>2</sub>  $<1$  wt.%. Therefore the telescopic and Clementine data indicate that the presence of the Airy albedo feature cannot be attributed to an unusual composition.

[10] We examined Clementine color (415-nm/750-nm ratio) and OMAT trends around the Airy albedo anomaly. The bright portions of the swirl have high OMAT and color ratio values, similar to those of small fresh craters in the vicinity. This is consistent with the presence of immature regolith. The central darker lane within the Airy albedo feature has OMAT and color ratio values that are lower than the bright portions, but are not as low as the values for mature surfaces in this region away from the magnetic anomaly. It may be that swirl dark lanes represent areas receiving enhanced solar wind flux because of scattering or focusing from the magnetically shielded areas [e.g., *Hood and Williams*, 1989].

#### 4. Discussion

[11] The Airy albedo feature consists of an elongated, curved bright area with a central darker lane. This marking, while not possessing the intricate swirl morphology of the RGF, is more complex than an albedo anomaly in the Descartes Formation south of the Apollo 16 site that is co-located with a magnetic anomaly [*Richmond et al.*, 2003; *Blewett et al.*, 2005]. The Descartes albedo feature is a simple bright patch, though the magnetic anomaly at the Descartes location is stronger than that at either RGF or Airy, with a two-dimensionally smoothed peak total field strength at 35.5 km altitude of  $>10$  nT.

[12] We have identified a progression in the morphology of albedo features that are located in areas of crustal magnetic anomalies. At one extreme are the complex looped and sinuous structures of the classic RGF-type swirl. Other examples of this level of complexity are the swirls in Mare Marginis and Mare Ingenii. The Descartes feature represents the other end of the continuum: a bright patch with diffuse edges. In between are intermediate forms such

as the single loop and dark lane of the Airy feature, perhaps an incipient swirl. Another occurrence of an intermediate form is in the farside highlands near crater Gerasimovich, where bright patches with some simple loops and dark lanes are found.

[13] Based on these examples, it appears that a strong magnetic anomaly at a mare location is likely to correlate with the complex swirl morphology characteristic of the RGF. Strong magnetic anomalies in the highlands are associated with high albedo features that display less well-developed swirl structure. We plan to conduct further study of these and other magnetic anomalies, focusing on mare/highland differences, the effect of both spatial extent and strength of the magnetic anomaly, and a detailed comparison of the spectral properties of swirl, dark lane, and normal background material. New data from upcoming lunar missions including Chandrayaan, Lunar Reconnaissance Orbiter, Chang'e-1, and SELENE (Kaguya) will be extremely valuable as we work to better understand the puzzle of the lunar swirls and the nature of space weathering on the airless rocky bodies of the Solar System.

[14] **Acknowledgments.** The authors thank the U. S. Geological Survey for maintaining the Map-A-Planet website and the Lunar and Planetary Institute for its on-line Lunar Atlases. The NASA Planetary Geology & Geophysics and Discovery Data Analysis Programs funded this work. C. G. H. appreciates the support from a NASA Planetary Geology & Geophysics Undergraduate Research Program internship that allowed him to spend a summer at NovaSol. Reviews by L. Hood and K. Hemant helped to improve this paper. This is HIGP publication 1506, SOEST paper 7196, and PSI contribution 423.

#### References

- Bell, J. F., and B. R. Hawke (1981), The Reiner Gamma Formation: Composition and origin as derived from remote sensing observations, *Proc. Lunar Planet. Sci. Conf.*, 12th, 679–694.
- Blewett, D. T., B. R. Hawke, P. G. Lucey, G. J. Taylor, R. Jaumann, and P. D. Spudis (1995), Remote sensing and geologic studies of the Schiller-Schickard region of the Moon, *J. Geophys. Res.*, 100, 16,959–16,977.
- Blewett, D. T., B. R. Hawke, and P. G. Lucey (2005), Lunar optical maturity investigations: A possible recent impact crater and a magnetic anomaly, *J. Geophys. Res.*, 110, E04015, doi:10.1029/2004JE002380.
- El-Baz, F. (1972), The Alhazen to Abul Wafa swirl belt: An extensive field of light-colored, sinuous markings, *NASA Spec Publ.*, SP-315.
- Grier, J. A., A. S. McEwen, P. G. Lucey, M. Milazzo, and R. G. Strom (2001), The optical maturity of ejecta from large rayed lunar craters, *J. Geophys. Res.*, 106, 32,847–32,862.
- Hapke, B. (2001), Space weathering from Mercury to the asteroid belt, *J. Geophys. Res.*, 106, 10,039–10,073.
- Hood, L. L., and N. A. Artemieva (2007), Antipodal effects of lunar basin-forming impacts: Initial 3D simulations and comparisons with observations, *Icarus*, doi:10.1016/j.icarus.2007.08.023, in press.
- Hood, L., and G. Schubert (1980), Lunar magnetic anomalies and surface optical properties, *Science*, 208, 49–51.
- Hood, L., and C. Williams (1989), The lunar swirls: Distribution and possible origins, *Proc. Lunar Planet. Sci. Conf.*, 19th, 99–113.
- Hood, L. L., A. Zakharian, J. Halekas, D. L. Mitchell, R. P. Lin, M. H. Acuna, and A. B. Binder (2001), Initial mapping and interpretation of lunar crustal magnetic anomalies using Lunar Prospector magnetometer data, *J. Geophys. Res.*, 106, 27,825–27,839.
- Lin, R. P., K. A. Anderson, and L. Hood (1988), Lunar surface magnetic field concentrations antipodal to young large impact basins, *Icarus*, 74, 529–541.
- Lucey, P. G., B. R. Hawke, C. M. Pieters, J. W. Head, and T. B. McCord (1986), A compositional study of the Aristarchus region of the Moon using near-infrared reflectance spectroscopy, *Proc. Lunar Planet. Sci. Conf.*, 16th, Part 2, *J. Geophys. Res.*, 91, D344–D354, suppl.
- Lucey, P. G., D. T. Blewett, and B. L. Jolliff (2000a), Lunar iron and titanium abundance algorithms based on final processing of Clementine UVVIS data, *J. Geophys. Res.*, 105, 20,297–20,306.
- Lucey, P. G., D. T. Blewett, G. J. Taylor, and B. R. Hawke (2000b), Imaging of lunar surface maturity, *J. Geophys. Res.*, 105, 20,377–20,386.

- McCord, T. B., R. N. Clark, B. R. Hawke, L. A. McFadden, P. D. Owensby, C. M. Pieters, and J. B. Adams (1981), Moon: Near-infrared spectral reflectance, A first good look, *J. Geophys. Res.*, *86*, 10,883–10,892.
- Nicholas, J. B., M. E. Purucker, and T. J. Sabaka (2007), Age spot or youthful marking: Origin of Reiner Gamma, *Geophys. Res. Lett.*, *34*, L02205, doi:10.1029/2006GL027794.
- Noble, S. K., and C. M. Pieters (2003), Space weathering on Mercury: Implications for remote sensing, *Astron. Vestnik*, *37*, 34–39.
- Pinet, P., V. Shevchenko, S. Chevrel, Y. Daydou, and C. Rosemberg (2000), Local and regional lunar regolith characteristics at Reiner Gamma Formation: Optical and spectroscopic properties from Clementine and Earth-based data, *J. Geophys. Res.*, *105*, 9457–9475.
- Richmond, N. C., and L. L. Hood (2007), A preliminary global map of the vector lunar crustal magnetic field based on Lunar Prospector magnetometer data, *J. Geophys. Res.*, doi:10.1029/2007JE002933, in press.
- Richmond, N. C., L. L. Hood, J. S. Halekas, D. L. Mitchell, R. P. Lin, M. Acuna, and A. B. Binder (2003), Correlation of a strong lunar magnetic anomaly with a high-albedo region of the Descartes mountains, *Geophys. Res. Lett.*, *30*(7), 1395, doi:10.1029/2003GL016938.
- Richmond, N. C., L. L. Hood, D. L. Mitchell, R. P. Lin, M. H. Acuna, and A. B. Binder (2005), Correlations between magnetic anomalies and surface geology antipodal to lunar impact basins, *J. Geophys. Res.*, *110*, E05011, doi:10.1029/2005JE002405.
- Schultz, P. H., and L. J. Srnka (1980), Cometary collisions with the Moon and Mercury, *Nature*, *284*, 22–26.
- Starukhina, L., and Y. Shkuratov (2004), Swirls on the Moon and Mercury: Meteoroid swarm encounters as a formation mechanism, *Icarus*, *167*, 136–147.
- Stöffler, D., H. Knoll, U. Marvin, C. Simonds, and P. Warren (1980), Recommended classification and nomenclature of lunar highland rocks—A committee report, in *Proceedings of the Conference on Lunar Highlands Crust*, pp. 51–70, Elsevier, New York.
- 
- D. T. Blewett, John Hopkins University Applied Physics Laboratory, Laurel, MD 20723, USA. (david.blewett@jhuapl.edu)
- B. R. Hawke, Hawai'i Institute of Geophysics and Planetology, University of Hawai'i, Honolulu, HI 96822, USA.
- C. G. Hughes, Department of Geology and Planetary Science, University of Pittsburgh, Pittsburgh, PA 15260, USA.
- N. C. Richmond, Planetary Science Institute, 1700 East Fort Lowell, Suite 106, Tucson, AZ 85719, USA.